Structure-Guided Design of *N*-Phenyl Tertiary Amines as Transrepression-Selective Liver X Receptor Modulators with Anti-Inflammatory Activity

Esther Y. Chao,[†] Justin A. Caravella, Mike A. Watson, Nino Campobasso,[†] Serena Ghisletti,[‡] Andrew N. Billin,[†] Cristin Galardi,[†] Ping Wang,[†] Bryan A. Laffitte, Marie A. Iannone,[†] Bryan J. Goodwin,[†] Jason A. Nichols,[†] Derek J. Parks,[†] Eugene Stewart,[†] Robert W. Wiethe,[†] Shawn P. Williams,[†] Angela Smallwood,[†] Kenneth H. Pearce,[†] Christopher K. Glass,[‡] Timothy M. Willson,[†] William J. Zuercher,[†] and Jon L. Collins*[,†]

GlaxoSmithKline Research and Development, Research Triangle Park, North Carolina 27709, and Departments of Cellular and Molecular Medicine and Medicine, School of Medicine, University of California, La Jolla, San Diego, California 92093

Received May 22, 2008

A cocrystal structure of T1317 (**3**) bound to hLXRβ was utilized in the design of a series of substituted *N*-phenyl tertiary amines. Profiling in binding and functional assays led to the identification of LXR modulator GSK9772 (**20**) as a high-affinity LXRβ ligand (IC_{50} = 30 nM) that shows separation of anti-inflammatory and lipogenic activities in human macrophage and liver cell lines, respectively. A cocrystal structure of the structurally related analog **19** bound to LXRβ reveals regions within the receptor that can affect receptor modulation through ligand modification. Mechanistic studies demonstrate that **20** is greater than 10-fold selective for LXR-mediated transrepression of proinflammatory gene expression versus transactivation of lipogenic signaling pathways, thus providing an opportunity for the identification of LXR modulators with improved therapeutic indexes.

Introduction

Liver X receptors (LXR)[a] α and β are ligand-activated transcription factors that belong to the nuclear receptor superfamily of hormone receptors. The identification of oxysterols, which is exemplified by 24(*S*),25-epoxycholesterol (**1**),[1,2] as natural LXR ligands as well as **2** (GW3965)[3] and **3** (T1317)[4] as synthetic, nonsteroidal LXR agonists facilitated the discovery of biological signaling pathways that are regulated by LXRs.[5−8] The LXRs regulate the expression of key target genes that are involved in cholesterol metabolism and transport (*abca1*, *abcg1*, *cyp7a*), glucose metabolism (*pepck*, *g6p*), and inflammation (*IL-6*, *inos*, *cox2*). These effects are manifested in vivo because **2** and **3** show beneficial effects in animal models of antiatherosclerosis, diabetes, inflammation, and neurodegenerative diseases. However, the beneficial effects of LXR agonists are compromised by the LXR-dependent increase in the expression of genes that control hepatic lipogenesis including *srebp1c* and *fas*. As a direct consequence, the chronic treatment of rodents with first-generation LXR agonists **2** and **3** leads to the accumulation of hepatic triglycerides and, with **2**, the elevation of low-density lipoprotein (LDL) particles in primates.[4,9] There is a clear need for LXR modulators that show the beneficial effects on cholesterol transport and inflammation but do not induce hepatic lipogenesis.

Chart 1. Structures of 24(*S*),25-Epoxycholesterol **1**, **2**, and **3**

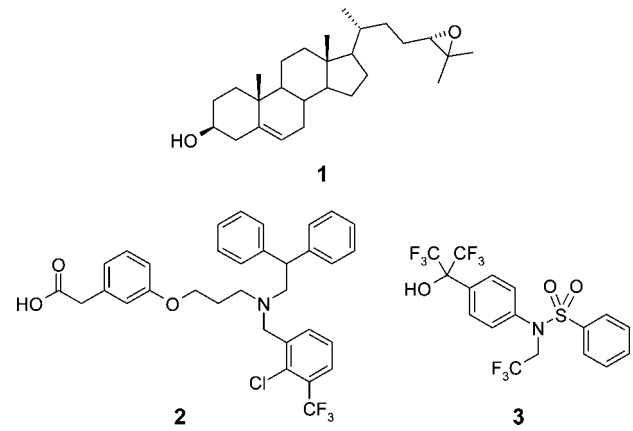

The crystal structures of **1**−**3** bound to the LXRs reveal large plastic ligand-binding pockets (LBPs) that vary in size and shape depending on the nature of the ligand.[10] The cumulative data from these structural studies suggest that the mechanism of receptor activation of the different ligands involves a conserved ligand-guided interaction between His^{435} on helix 10/11 and a Trp^{457} on the activation function-2 (AF-2) helix. This interaction stabilizes the position of the AF-2 helix against the LBP, which leads to a transcriptionally active receptor. Three key observations were noted in the cocrystal structure of **3** bound to LXRβ. First, the acidic bistrifluoromethyl alcohol in **3** was involved in a strong hydrogen-bond interaction with His^{435}, which suggests that this interaction is critical for ligand binding and receptor activation. Second, the sulfonyl moiety was not involved in an interaction with residues that line the LBP, which suggests that the replacement of this group with a methylene would not dramatically reduce the binding affinity. Third, syn and anti conformations around the tertiary sulfonamide bond were observed in different unit cells of the cocrystal structure, which

* To whom correspondence should be addressed. Address: Five Moore Drive, North-1510, Research Triangle Park, NC 27709. Phone: 919-483-5694. Fax: 919-315-0430. E-mail: Jon.L.Collins@gsk.com.

[†] GlaxoSmithKline Research and Development.

[‡] Departments of Cellular and Molecular Medicine and Medicine, University of California.

[a] Abbreviations: LXR, liver X receptor; *abca1/g1*, adenosine triphosphate binding cassette a/g; *cyp7a*, cytochrome P450 7a hydroxylase; *pepck*, phosphoenolpyruvate carboxykinase; *g6p*, glucose-6-phosphate; IL-6, interleukin-6; *inos*, inducible nitric oxide synthase; *cox2*, cyclooxygenase 2; *srebp1c*, sterol regulatory element binding protein-1c; *fas*, fatty acid synthase; LBP, ligand-binding pocket; LBD, ligand-binding domain; NPTA, *N*-phenyl tertiary amine; DMAP, 4-dimethylaminopyridine; Et_3N, triethylamine; $NaHB(OAc)_3$, sodium triacetoxyborohydride; LAH, lithium aluminum hydride; DMF, *N*,*N*-dimethylformamide; AF-2, activation function-2; SUMO, small ubiquitin-like modifier; SRC-1, steroid receptor coactivator-1; NCoR, nuclear receptor repressor; ChIP, chromatin immunoprecipitation.

10.1021/jm800612u CCC: $40.75
Published on Web 08/23/2008

Scheme 1[a]

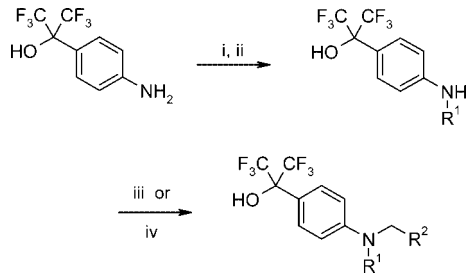

[a] Reagents: (i) $R^1C(O)OC(O)R^1$, Et_3N, DMAP, DCM; (ii) LAH, Et_2O; (iii) R^2CHO, $NaBH(OAc)_3$, AcOH, DCE; or (iv) R^2CH_2X, DMF, 140°C, microwave.

indicates that this region of the pocket was quite plastic. These three observations led us to explore modifications of **3** that would perturb the receptor conformation and potentially lead to dissociated functional activities.

Chemistry

Commercially available 2-(4-aminophenyl)-1,1,1,3,3,3-hexafluoropropan-2-ol was converted to an amide following treatment with an acyl anhydride, Et_3N, and DMAP (Scheme 1) and was reduced with LAH to provide an intermediate secondary aniline. Subjection of the product aniline to $NaBH(OAc)_3$ and AcOH in the presence of aldehydes gave rise to substituted *N*-phenyl tertiary amines (NPTAs) in good overall yield and purity. Alternatively, the intermediate secondary aniline was alkylated with benzyl halides in DMF while heating in a microwave. Both procedures proved to be very efficient for the preparation of the targeted *N*-phenyl tertiary amines. Compound **6** was prepared according to the published procedure.[11]

Results and Discussion

The targeting of the classical nuclear receptor ligand−AF-2 helix interaction has proven to be an effective strategy for the conversion of full agonists to partial agonists and antagonists.[12,13] On the basis of this, our initial efforts focused on determining whether one of the bistrifluoromethyl groups in **3** could be replaced with hydrophobic groups of different size, shape, and directionality. Simple replacement of one of the bis-trifluoromethyl groups with small substituted or unsubstituted aliphatic, aryl, or alkyne groups led to only weak partial LXR agonism (data not shown), which reinforced our hypothesis that the acidic bistrifluoromethyl alcohol−His^{435}−Trp^{457} triad would be required for high-affinity binding to LXR. These results prompted us to design and synthesize analogs that retain the bistrifluoromethyl benzyl alcohol pharmacophore of **3** yet contain a replacement of the tertiary sulfonamide moiety with substituted *N*-phenyl tertiary amines.

The cocrystal structure of **3** bound to LXRβ suggested that the trifluoroethyl group could be replaced with small hydrophobic groups. The syn conformer of **3** occupied a hydrophobic pocket; in contrast, the anti conformer occupied a polar region within the LBP. An initial set of compounds was prepared from small alkyl anhydrides and aryl/heteroaryl aldehydes. Screening in LXRα and LXRβ competitive binding assays provided several potent dual LXRα/β ligands (Table 1, compounds **4**−**12**). Whereas an *N*-butyl group was the preferred *N*-alkyl substituent, the benzenesulfonyl moiety could be replaced by various benzyl, substituted-benzyl, and heteroaryl (pyridine, furan, thiophene) groups, suggesting that this region of the LBP could accommodate a variety of *N*-benzyl substitutions. We previously reported that LXR agonists show anti-inflammatory

Table 1. LXR Modulator Profile of *N*-Phenyl Tertiary Amines[a,b]

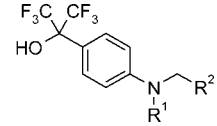

			binding		functional		
			LXRα	LXRβ	IL-6 ELISA		TG
cmpd	R^1	R^2	IC_{50}	IC_{50}	IC_{50}	RE	RE
2			235	30	20	1.0	1.0
3			75	30	100	1.0	1.0
4	Me	Ph	310	170	NT	NT	>0.5
5	*n*-Bu	Ph	170	40	25	1.0	0.8
6	Bn	Ph	315	175	NT	NT	>0.5
7	*n*-Bu	3-$HOCH_2CH_2$-Ph	115	15	5	1.0	1.8
8	*n*-Bu	2-pyridyl	120	30	20	1.0	1.1
9	*n*-Bu	4-pyridyl	90	25	20	1.0	1.1
10	*n*-Bu	2-HO-Ph	180	40	35	1.0	0.6
11	*n*-Bu	3-HO-Ph	160	30	35	1.0	0.5
12	*n*-Bu	4-HO-Ph	955	740	NT	NT	NT
13	*n*-Bu	2-HO-3-F-Ph	615	120	60	1.0	1.9
14	*n*-Bu	2-HO-5-CF_3O-Ph	190	165	NT	NT	1.0
15	*n*-Bu	2-HO-3,5-Cl_2-Ph	890	290	1290	<0.5	ia
16	*n*-Bu	2-HO-5-Cl-Ph	220	115	55	1.0	1.0
17	*n*-Bu	3-Cl-4-HO-Ph	560	50	25	1.0	0.6
18	*n*-Bu	3-Cl-4-HO-5-MeO-Ph	775	45	10	1.0	<0.2
19	*n*-Bu	3-Cl-4,5-$(OMe)_2$-Ph	165	25	15	1.0	0.4
20	*n*-Bu	3-,5-Cl_2-4-HO-Ph	180	30	15	1.0	<0.1
21	*n*-Bu	3,5-Cl_2-Ph	195	30	10	1.0	0.7
22	*n*-Bu	3,5-Cl_2-4-MeO-Ph	170	30	15	1.0	0.8

[a] IC_{50} data are in nM and are expressed as the mean of ≥3 replicates (variation <25%). RE is relative efficacy compared with **2**, **3**, or both. NT is not tested. [b] TG RE data were determined by dose-response testing up to 10 μM test concentration and are expressed relative to **2**, **3**, or both (≥3 replicates).

and lipogenic activities in IL-6 ELISA and triglyceride accumulation assays, respectively.[14] Compounds **4**−**12** were profiled in these functional assays to determine whether substituted NPTAs would show a differential profile relative to **3**. Analogs containing an unsubstituted phenyl (compound **5**), pyridine (compounds **8** and **9**), or hydroxyethyl ether (**7**) did not show a significant separation of anti-inflammatory and lipogenic activity. In contrast, NPTAs **10** and **11**, which contained a phenol substituent, consistently showed anti-inflammatory activity that was comparable to that of **3** and only partial (50−60%) induction of triglyceride accumulation.

In an attempt to explore the SAR of LXR modulation and to reduce lipogenic activity further, a second set of analogs was prepared wherein the *N*-butyl group was maintained and variations were made to the benzyl group. Screening of the analogs in competitive binding assays provided several high-affinity LXRβ ligands that contained phenols and phenolic ethers (compounds **13**−**20**). The preference for *o*- and *m*-phenols over *p*-phenols for derivatives **10**−**12** was reversed with more highly substituted analogs **13**−**20**; *p*-phenols showed a higher affinity for the latter. Functional profiling of **13**−**20** in anti-inflammatory and triglyceride accumulation assays revealed that LXRβ binding affinity generally correlated with the inhibition of IL-6 secretion but not with lipogenic potential. With the exception of **13**, the majority of these NPTA analogs showed reduced lipogenic potential relative to that of **3**. Of these, **20** dose-dependently inhibited IL-6 secretion (IC_{50} = 15 nM) but did not induce triglyceride accumulation in a human liver cell line (Table 1, Figure 1A,B). Interestingly, analogs that lacked a phenol group (**21**) or contained a methyl ether (**22**) showed increased lipogenic potential compared with **20**, which suggests that the phenol is critical for receptor modulation. To address whether metabolism could explain the differential profile with

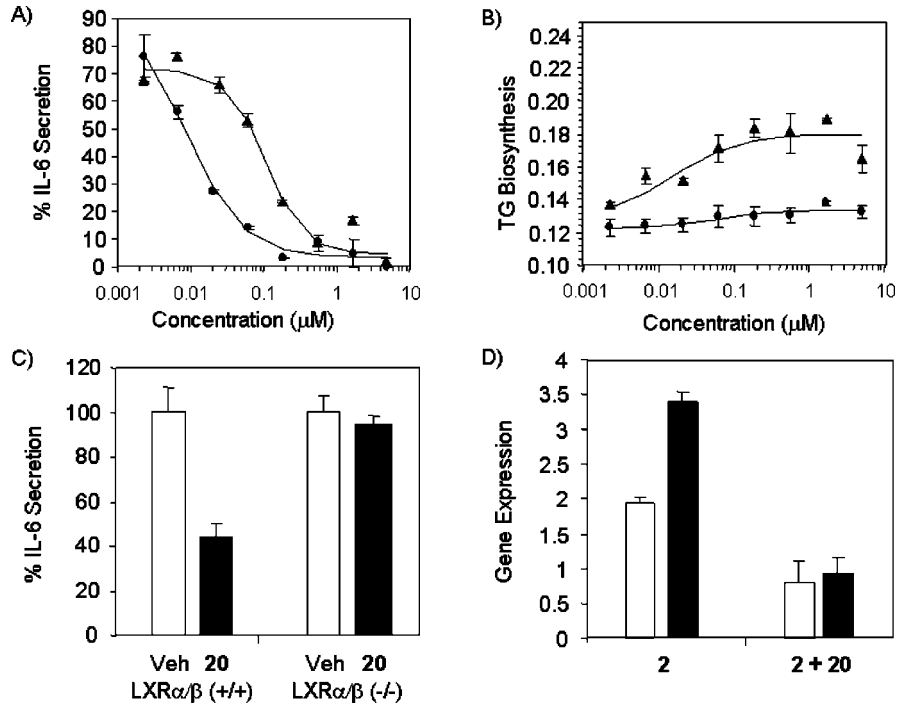

Figure 1. Effects of **3** (▲) and **20** (●) on (A) LPS-stimulated IL-6 secretion in THP-1 cells and (B) triglyceride accumulation in HuH7 cells. (C) Effects of vehicle (open bars) and **20** (1 μM, solid bars) on LPS-induced IL-6 secretion in peritoneal macrophages that were isolated from wild-type vs LXRα/β knockout mice. (D) Induction of *srebp1c* (open bars) and *fas* (solid bars) mRNA expression in HepG2 cells by **2** (200 nM) alone or in the presence of **20** (500 nM). Data are expressed as fold expression over vehicle-treated cells. The data are the average of ≥ 3 replicates.

20, we determined the percentage of parent compound that remained in HuH7 cells under conditions that were used for the triglyceride accumulation assay. After being dosed at 1 μM and incubated for 24 h, compounds **3** and **20** showed 65 and 40% of parent compound remaining, respectively, which suggests that the unique profiles were not due to differential metabolism. Therefore, **20** (GSK9772) is a high-affinity LXR modulator that dissociates anti-inflammatory signaling from lipogenic signaling.

Compound **20** was characterized in nuclear receptor selectivity and functional assays to support our hypothesis further that the dissociated activities were LXR-dependent (Figure 1). With the exception of full-length human PXR ($EC_{50} = 250$ nM), **20** was 100-fold selective when screened in a panel of nuclear receptor selectivity assays including AR, GR, PR, MR, ERα/β, FXR, and PPAR$\alpha/\gamma/\delta$ (data not shown). The dissociated profile with **20** would not be due to PXR cross reactivity because PXR agonists do not affect IL-6 secretion or triglyceride accumulation. Importantly, the ability of **20** to repress IL-6 secretion from peritoneal macrophages of wild-type mice was completely abolished in macrophages that were derived from LXR-null mice (Figure 1C). Moreover, compound **20** effectively antagonized the LXR agonist-induced expression of the lipogenic genes *srebp1c* and *fas* in HuH7 cells (Figure 1D). The cumulative data from these experiments confirm that the dissociation of anti-inflammatory signaling from lipogenic signaling by **20** is indeed LXR-dependent.

The design of NPTAs as LXR modulators that are centered around the bistrifluoromethyl alcohol moiety is a key pharmacophore for high-affinity binding to the LXRs. Because of the proximity of this functional group to the cofactor−AF-2 interface, compounds **3**, **19**, and **20** were profiled in cell-free and cellular cofactor−LXRα/β interaction assays to probe whether differential cofactor peptide recruitment could explain the dissociated activities. No significant differences were observed when the compounds were screened in cell-free fluorescent resonance energy transfer (FRET) assays that used peptide fragments from the steroid receptor coactivator-1 (SRC-1) and nuclear corepressor (NCoR).[3] Moreover, the screening of **3**, **19**, and **20** in cell-free multiplexed peptide interaction assays that used a panel of 90 coactivator and corepressor peptide fragments (21- to 26-mer) did not differentiate the three compounds (Figure 2A).[15,16] In contrast, significant differences between **3** and **20** were observed upon the screening in cellular mammalian two-hybrid (M2H) assays that used longer peptide fragments of SRC-1 (190 amino acids) and NCoR (61 amino acids) (Figure 2B). Whereas **3** effectively recruited SRC-1 and effectively displaced NCoR, LXR modulator **20** was significantly less potent at recruiting SRC-1 and did not displace NCoR from the LXR ligand-binding domain (LBD), which suggests that **20** binds and stabilizes the LXR in an NCoR-associated, repressed state.

In an attempt to explore the structural basis for this finding, we solved the cocrystal structure of **19** bound to mLXRα to 2.35 Å resolution (Figure 3). The binding orientation was very similar to that of the anti conformer of the LXR agonist **3** with the bistrifluoromethyl alcohol directed toward AF-2. Consistent with cell-free cofactor recruitment data, the positions of the AF-2 helix in both cocrystal structures were nearly identical. A difference in the structure of **19** was the presence of a hydrogen bond between the 4-methoxy group of **19** and Ser^{262} of LXR. It is interesting that relatively minor changes in this region of the ligand can significantly alter the effect on triglyceride accumulation. (See the results for ligands **17**−**22** in Table 1.) For example, compound **20** contains a 4-phenol that also would be expected to hydrogen bond with Ser^{262}. In contrast, compound **21**, which lacks a 4-phenol, shows much higher triglyceride accumulation than does **20**. The substituents in this region do, however, appear to affect the conformation of the loop between helices 5 and 6. Whereas no firm crystal structure−

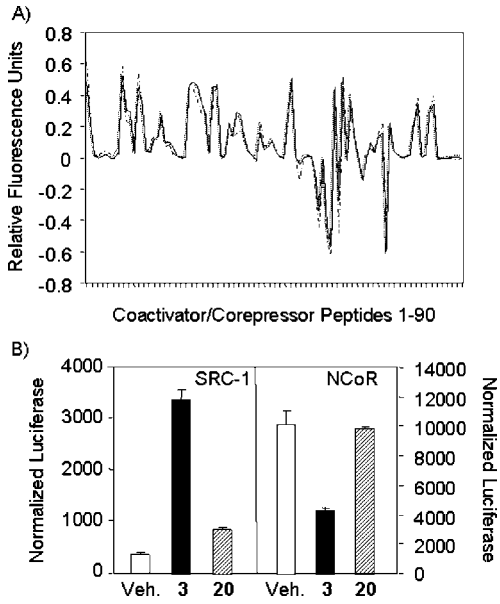

Figure 2. (A) Profiling of **3**, **19**, and **20** in cell-free multiplexed peptide interaction assays by the use of a panel of 90 coactivator and corepressor peptide fragments that ranged from 21 to 26 amino acids. Data are expressed as log fluorescence units (peptide + compound/peptide basal) ($n = 4$). Nearly identical profiles were observed for the three LXR ligands. (B) Screening of **3** and **20** (5 μM) in cellular mammalian two-hybrid assays that used fragments of SRC-1 (190 amino acids) and NCoR (61 amino acids) revealed significant differences between **3** and anti-inflammatory LXR modulator **20**.

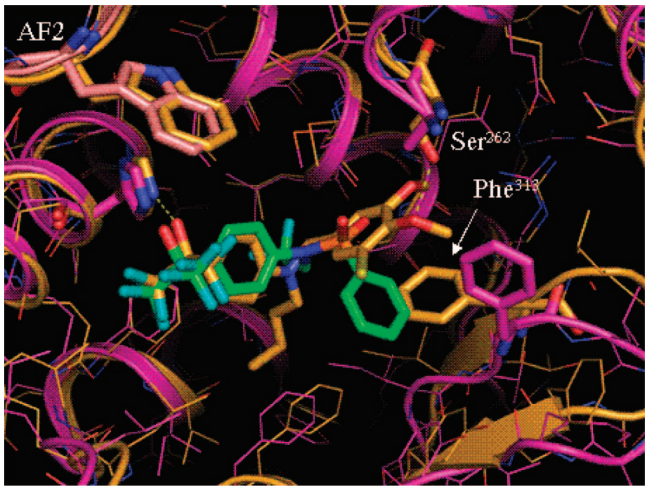

Figure 3. Crystal structure of **3** (green, gauche conformer) bound to hLXRβ (magenta). The AF-2 helix is highlighted in pink. The cocrystal structure of **19** bound to mLXRα is superimposed and shown in orange. A hydrogen-bond interaction between the bistrifluoromethyl alcohol of **19** and His^{419} of helix 10/11 is similar to that seen in the complex with **3**. There is also a hydrogen bond between Ser^{262} and the 4-methoxy group of **19**. The conformation of the loop, particularly Phe^{313}, between helices 5 and 6 of the receptor (lower right) appears to be dramatically influenced by the substituents on the phenyl ring of **19**.

functional-activity relationship could be gleaned from the **19**-LXR cocrystal structure, the crystallographic data coupled with the M2H data suggest that regions of the receptor that are distal from the coactivator peptide-binding site can modulate corepressor interaction and LXR functional activity.

Mechanism of Anti-inflammatory versus Lipogenic Activities. The identification of **20** provided a chemical tool to explore the mechanistic basis for the differential effects in anti-inflammatory versus lipogenic assays. The mechanistic basis

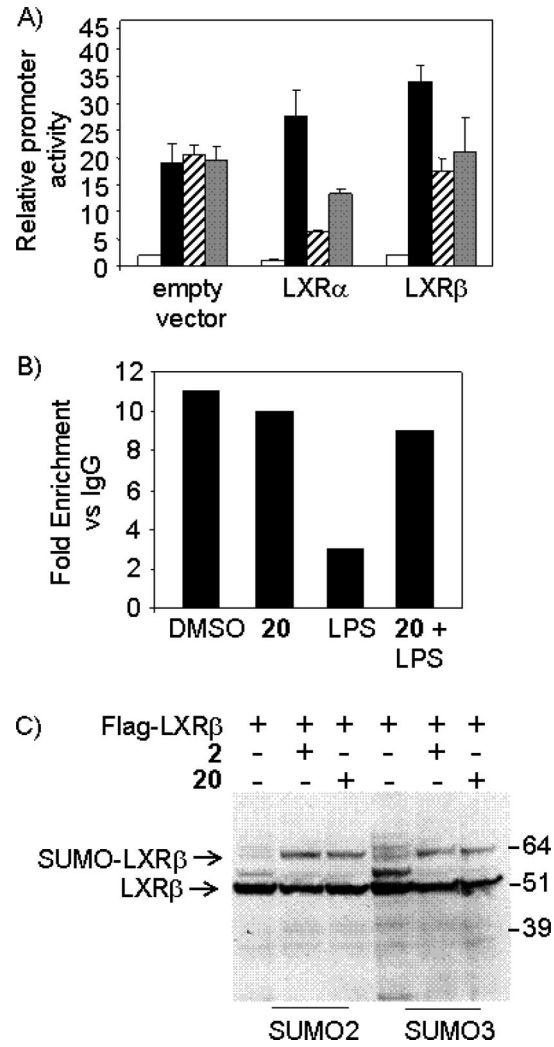

Figure 4. (A) Transrepression of LPS-induced (black bar) *inos* promoter activation in RAW264.7 cells with **2** (1 μM, hatched bar) and **20** (1 μM, gray bar) in the absence and presence of LXRα and LXRβ. (B) ChIP analysis using antibody against NCoR (vs IgG control) of LPS-treated primary macrophages in the absence and presence of **20** (1 μM). Immunoprecipitated DNA was analyzed by real-time PCR using primers that were specific for the *inos* promoter. (C) LXRβ is SUMOylated by SUMO2 and SUMO3 upon treatment with **2** (1 μM) and **20** (1 μM) in HeLa cells. Whole cell lysates were immunoblotted for FLAG tag.

of the repression of gene expression, designated transrepression, has been poorly understood. Recent literature data has demonstated that the LXRs transrepress LPS-induced proinflammatory gene expression (*IL-6*, *inos*) by the ligand-dependent SUMOylation of lysine residues that are contained in the LBD, which results in the targeting of SUMO−LXR to promoters of inflammatory genes, the inhibition of NCoR clearance from the promoters, and the repression of proinflammatory gene expression.[17,18] To test whether *N*-phenyl tertiary amines transpress via a similar mechanism, **20** was evaluated in LPS-treated reporter gene transrepression, SUMOylation, and chromatin immunoprecipitation (ChIP) assays (Figure 4). Whereas **2** and **20** did not show an effect in the iNOS promoter-driven reporter gene assay in the absence of LXRα or LXRβ, both compounds showed comparable repression of LPS-stimulated *inos* expression in the presence of both LXRα and LXRβ (Figure 4A). Morever, upon treatment with LPS, both compounds inhibited the clearance of NCoR from the *inos* promoter and induced the SUMOylation of LXRβ but not of LXRα (data

not shown) upon analysis in Western blot and NCoR ChIP assays (Figure 4B,C), respectively, which demonstrates that **20** shows anti-inflammatory activity via a mechanism that is similar to that of the first-generation LXR ligand **2**.

First-generation LXR ligands increase the expression of target genes through a complex series of events: designated transactivation, which includes ligand binding, heterodimerization with RXR, DNA binding, coactivator recruitment, and assembly of cellular transcriptional machinery. The ability of **3** and **20** to transactivate target genes differentially was determined by profiling in reporter gene functional assays. Consistent with the relatively weak recruitment of the coactivator SRC-1 (Figure 2B) and the minimal induction of the lipogenic genes *srebp1c* and *fas* (Figure 1D), **20** showed very weak ($EC_{50} = 3-5$ uM) transactivation potential when it was tested in cell-based LXRα− and LXRβ−GAL4 reporter gene expression assays and only weakly induced the reverse cholesterol transport pathway via ABCA1 (data not shown).[3] Overall, the cumulative data suggest that the mechanism of anti-inflammatory activity versus lipogenic activity with **20** results from the greater than 10-fold selectivity for the transrepression of anti-inflammatory target genes versus the transactivation of lipogenic genes.

Conclusions

The **3**-LXRβ cocrystal structure led to the design and synthesis of a series of *N*-phenyl tertiary amines. Profiling in binding and functional assays led to the discovery of **20** as an LXR modulator that shows potent anti-inflammatory activity but does not induce the expression of lipogenic genes or hepatic triglyceride accumulation. Cofactor profiling revealed key differences between first-generation LXR agonist **3** and **20** by the use of M2H profiling assays with more than 60 amino acid fragments of SRC-1 and NCoR, which suggests that **20** stabilizes LXR in a basal, repressed state. An NPTA−LXR cocrystal structure revealed unexpected regions within the LXR ligand-pocket that affect receptor conformation and functional activity. Importantly, in vitro receptor profiling with 15- to 21-mer peptides was not able to differentiate the phenotype of receptor modulation distal to the AF-2 helix. Our results define the limitations of short coactivator and corepressor peptide profiling for the characterization and optimization of NR modulators. Whereas compounds that directly affect AF-2 can be binned by the use of these technologies,[16,19] we now demonstrate that compounds that modulate receptor function distal to AF-2 require large coactivator and corepressor fragments to distinguish their pharmacology. Mechanistic studies showed that **20**, like first-generation LXR agonist **2**, effectively suppressed the expression of proinflammatory target genes via a SUMOylation-dependent mechanism, which resulted in a greater than 10-fold selectivity for transrepression versus transactivation. LXR modulator **20** will serve as a valuable chemical tool for exploring nuclear receptor transrepression and will provide an opportunity for the future discovery of LXR modulators with improved therapeutic indexes.

Experimental Section

1,1,1,3,3,3-Hexafluoro-2-{4-[methyl(phenylmethyl)amino]phenyl}-2-propanol (4). A solution of 2-(4-aminophenyl)-1,1,1,3,3,3-hexafluoro-2-propanol (101 mg, 0.39 mmol) in 0.8 mL of MeOH/trimethyl orthoformate (1:1) at 25 °C was treated with benzaldehyde (40 μL, 0.39 mmol). After being stirred overnight, the reaction was treated with solid $NaBH_4$ in small portions until TLC indicated that the intermediate imine was consumed. The reaction was filtered through a pad of silica gel with EtOAc as the eluent, and the filtrate was concentrated in vacuo. Purification by SiO_2 chromatography (4:1 hexanes/EtOAc) provided 85 mg (63%) of an intermediate secondary amine. A solution of 60 mg (0.17 mmol) of the intermediate in 600 μL of glacial acetic acid was treated with excess paraformaldehyde followed by 53 mg (0.85 μmol) of $NaCNBH_3$. After being stirred at room temperature for 15 h, the reaction was filtered through silica gel with EtOAc as the eluent, and the filtrate was concentrated in vacuo. Purification by preparative TLC (SiO_2, 1000 μm) that used hexanes/EtOAc (4:1) provided 30 mg (50%) of **4**: ^{1}H NMR ($CDCl_3$, δ): 3.07 (s, 3H), 4.56 (s, 2H), 6.76 (d, J = 8.8 Hz, 2H), 7.18−7.29 (m, 3H), 7.33 (t, J = 7.4 Hz, 2H), 7.49 (d, J = 8.8 Hz, 2H). MS (ES) *m/e*: 364 (M + 1). >99% pure by HPLC (Waters symmetry shield, RPq 3.5 μm, 2.1 × 30 mm^2, H_2O/CH_3CN (85:15) with 0.1% HCOOH to 100% CH_3CN over 4 min, flow rate = 1.2 mL/min). t_R = 4.61 min. HRMS (ES+) *m/e*: (M + 1) calcd for $C_{17}H_{17}F_6N_1O$, 364.1136; found, 364.1131.

2-{4-[Butyl(pyridin-2-ylmethyl)amino]phenyl}-1,1,1,3,3,3-hexafluoropropan-2-ol (8). To a solution of 2-(bromomethyl)pyridine (0.06 g, 0.32 mmol) in 0.2 mL DMF were added 2-[4-(butylamino)phenyl]-1,1,1,3,3,3-hexafluoropropan-2-ol (0.05 g, 0.16 mmol) and K_2CO_3 (0.06 g, 0.48 mmol). The mixture was heated in a microwave at 140 °C for 15 min and was then evaporated to dryness. We purified the residue on a prep Agilent HPLC system with a Phenomenex Luna 5 μm C18 (150 × 21 mm) column by using 30−100% CH_3CN/H_2O that contained 0.1% TFA over 10 min to give compound **8**: ^{1}H NMR (CD_3OD, δ): 1.01 (t, 3H), 1.45 (m, 2H), 1.71 (m, 2H), 3.61 (t, 2H), 4.98 (s, 2H), 6.79 (d, J = 9.1 Hz, 2H), 7.54 (d, J = 8.8 Hz, 2H), 7.86 (t, 2H), 8.42 (t, 1H), 8.72 (d, J = 5.5 Hz, 1H). MS (APCI) *m/e*: 407 (M + 1). >99% pure by HPLC (Waters symmetry shield, RPq 3.5 μm, 2.1 × 30 mm^2, H_2O (with 0.1% HCOOH)/MeOH (with 0.075% HCOOH) (50:50) to 100% MeOH (with 0.075% HCOOH) over 5 min, flow rate = 1.0 mL/min, 210−400 nm). t_R = 3.13 min. HRMS (ES+) *m/e*: (M + 1) calcd for $C_{19}H_{21}F_6N_2O$, 407.1558; found, 407.1553.

2-{4-[Benzyl(butyl)amino]phenyl}-1,1,1,3,3,3-hexafluoropropan-2-ol (5). Step 1: To a solution of 2-(4-aminophenyl)-1,1,1,3,3,3-hexafluoropropan-2-ol (10 g, 0.04 mol) in 170 mL of DCM were added butyric anhydride (12 mL, 0.07 mol), triethylamine (14 mL, 0.09 mol), and catalytic DMAP. The mixture was heated to 40 °C for 18 h and was then evaporated to dryness. The residue was dissolved in ethyl acetate, treated with 10% K_2CO_3, and stirred at 25 °C for 2 h. A solid precipitated and was collected by filtration. The crude amide/ester was treated with 1 M LAH (95 mL, 0.095 mmol) in Et_2O and was then stirred at 25 °C for 4 h. The reaction was treated with H_2O (20 mL) at 0 °C, followed by 15% NaOH (50 mL) and was then filtered through celite. The mixture was extracted with EtOAc, and the organic layers were dried ($MgSO_4$), filtered, and evaporated to dryness to provide 9.5 g (75%) of 2-[4-(butylamino)phenyl]-1,1,1,3,3,3-hexafluoropropan-2-ol. ^{1}H NMR ($CDCl_3$, δ): 0.98 (t, 3H), 1.45 (m, 2H), 1.63 (m, 2H), 3.15 (t, 2H), 6.63 (dd, J = 1.9, 9.0 Hz, 2H), 7.45 (d, J = 8.7 Hz, 2H).

Step 2: To a solution of benzaldehyde (1.7 g, 15.9 mmol) in DCE (30 mL) were added glacial AcOH (1 mL), 2-[4-(butylamino)phenyl]-1,1,1,3,3,3-hexafluoropropan-2-ol (1 g, 3.2 mmol), and $NaHB(OAc)_3$ (4 g, 16 mmol). The mixture was stirred at 25 °C for 18 h and was then evaporated to dryness. The residue was purified on a prep Agilent HPLC system with a Phenomenex Luna 5 μm C18 (150 × 21 mm^2) column and was eluted with 30−100% CH_3CN/H_2O that contained 0.1% TFA over 10 min to give compound **5**. ^{1}H NMR (CD_3OD, δ): 0.97 (t, 3H), 1.41 (m, 2H), 1.65 (m, 2H), 3.49 (t, 2H), 4.62 (s, 2H), 6.76 (d, J = 9.0 Hz, 2H), 7.21−7.33 (m, 5H), 7.48 (d, J = 8.8 Hz, 2H). MS (APCI) *m/e*: 406 (M + 1). >99% pure by HPLC (Waters symmetry shield, RPq 3.5 μm, 2.1 × 30 mm^2, H_2O (with 0.1% HCOOH)/MeOH (with 0.075% HCOOH) (50:50) to 100% MeOH (with 0.075% HCOOH) over 5 min, flow rate = 0.8 mL/min, 210−400 nm). t_R = 4.27 min. HRMS (ES+) *m/e*: (M + 1) calcd for $C_{20}H_{22}F_6NO$ (M + 1); found, 406.1600.

Compounds Prepared in an Analogous Fashion. 2-(4-{Butyl[3-(2-hydroxyethoxy)benzyl]amino}phenyl)-1,1,1,3,3,3-hexafluoropropan-2-ol (7). ^{1}H NMR (CD_3OD, δ): 0.98 (t, 3H), 1.42 (m, 2H), 1.66 (m, 2H), 3.48 (t, 2H), 3.84 (t, 2H), 3.98 (t, 3H), 4.58 (s,

2H), 6.72 (d, J = 9.0 Hz, 2H), 6.81 (s, 1H), 6.82 (d, J = 6.9 Hz, 2H), 7.23 (t, 1H), 7.45 (d, J = 8.7 Hz, 2H). MS (APCI) *m/e*: 466 (M + 1). >97% pure by HPLC (Waters symmetry shield, RPq 3.5 μm, 2.1 × 30 mm^2, H_2O (with 0.1% HCOOH)/MeOH (with 0.075% HCOOH) (50:50) to 100% MeOH (with 0.075% HCOOH) over 5 min, flow rate = 0.8 mL/min, 210−400 nm). t_R = 4.26 min. HRMS (ES+) *m/e*: (M + 1) calcd for $C_{20}H_{22}F_6NO$, 466.1817; found, 466.1820.

2-{4-[Butyl(pyridin-4-ylmethyl)amino]phenyl}-1,1,1,3,3,3-hexafluoropropan-2-ol (9). ^{1}H NMR (CD_3OD, δ): 1.01 (t, 3H), 1.46 (m, 2H), 1.70 (m, 2H), 3.59 (t, 2H), 4.94 (s, 2H), 6.72 (d, J = 9.2 Hz, 2H), 7.50 (d, J = 8.7 Hz, 2H), 7.90 (d, J = 4.8 Hz, 2H), 8.74 (br s, 2H). MS (APCI) *m/e*: 407 (M + 1). >99% pure by HPLC (Waters symmetry shield, RPq 3.5 μm, 2.1 × 30 mm^2, H_2O (with 0.1% HCOOH)/MeOH (with 0.075% HCOOH) (50:50) to 100% MeOH (with 0.075% HCOOH) over 5 min, flow rate = 0.8 mL/min, 210−400 nm). t_R = 2.66 min. HRMS (ES+) *m/e*: (M + 1) calcd for $C_{19}H_{21}F_6N_2O$, 407.1558; found, 407.1553.

2-[(Butyl{4-[2,2,2-trifluoro-1-hydroxy-1-(trifluoromethyl)ethyl]phenyl}amino)methyl]phenol (10). ^{1}H NMR ($CDCl_3$, δ): 0.91 (t, 3H), 1.32 (m, 2H), 1.56 (m, 2H), 3.31 (t, 2H), 4.47 (s, 2H), 6.87 (m, 2H), 7.03 (d, J = 8.9 Hz, 2H), 7.18 (m, 2H), 7.59 (d, J = 8.7 Hz, 2H). MS (APCI) *m/e*: 422 (M + 1). >98% pure by HPLC (Waters symmetry shield, RPq 3.5 μm, 2.1 × 30 mm^2, H_2O (with 0.1% HCOOH)/MeOH (with 0.075% HCOOH) (50:50) to 100% MeOH (with 0.075% HCOOH) over 5 min, flow rate = 0.8 mL/min, 210−400 nm). t_R = 4.34 min. HRMS (ES+) *m/e*: (M + 1) calcd for $C_{20}H_{21}F_6NO_2$, 422.1555; found, 422.1549.

3-[(Butyl{4-[2,2,2-trifluoro-1-hydroxy-1-(trifluoromethyl)ethyl]phenyl}amino)methyl]phenol (11). ^{1}H NMR (CD_3OD, δ): 0.98 (t, 3H), 1.41 (m, 2H), 1.67 (m, 2H), 3.45 (t, 2H), 4.54 (s, 2H), 6.65−6.73 (m, 5H), 7.14 (m, 1H), 7.45 (d, J = 8.9 Hz, 2H). MS (APCI) *m/e*: 422 (M + 1). >99% pure by HPLC (Waters symmetry shield, RPq 3.5 μm, 2.1 × 30 mm^2, H_2O (with 0.1% HCOOH)/MeOH (with 0.075% HCOOH) (50:50) to 100% MeOH (with 0.075% HCOOH) over 5 min, flow rate = 0.8 mL/min, 210−400 nm). t_R = 4.27 min. HRMS (ES+) *m/e*: (M + 1) calcd for $C_{20}H_{21}F_6NO_2$, 422.1555; found, 422.1549.

4-[(Butyl{4-[2,2,2-trifluoro-1-hydroxy-1-(trifluoromethyl)ethyl]phenyl}amino)methyl]phenol (12). ^{1}H NMR (CD_3OD, δ): 0.89 (t, 3H), 1.25 (m, 2H), 1.51 (m, 2H), 3.08 (t, 2H), 3.88 (s, 2H), 6.73 (d, J = 8.4 Hz, 2H), 6.84 (d, J = 8.7 Hz, 1H), 6.99 (d, J = 8.4 Hz, 2H), 7.43 (s, 1H), 7.52 (d, J = 8.6 Hz, 1H). MS (ES) *m/e*: 422 (M + 1). >96% pure by HPLC (Waters symmetry shield, RPq 3.5 μm, 2.1 × 30 mm^2, H_2O (with 0.1% HCOOH)/MeOH (with 0.075% HCOOH) (50:50) to 100% MeOH (with 0.075% HCOOH) over 3.5 min, flow rate = 1.5 mL/min, 210−400 nm). t_R = 2.56 min. HRMS (ES+) *m/e*: (M + 1) calcd for $C_{20}H_{21}F_6NO_2$, 422.1555; found, 422.1549.

2-[(Butyl{4-[2,2,2-trifluoro-1-hydroxy-1-(trifluoromethyl)ethyl]phenyl}amino)methyl]-6-fluorophenol (13). ^{1}H NMR (CD_3OD, δ): 0.98 (t, 3H), 1.43 (m, 2H), 1.67 (m, 2H), 3.50 (t, 2H), 4.61 (s, 2H), 6.78 (m, 4H), 6.96 (m, 1H), 7.48 (d, J = 8.8 Hz, 2H). MS (APCI) *m/e*: 440 (M + 1). >96% pure by HPLC (Waters symmetry shield, RPq 3.5 μm, 2.1 × 30 mm^2, H_2O (with 0.1% HCOOH)/MeOH (with 0.075% HCOOH) (50:50) to 100% MeOH (with 0.075% HCOOH) over 5 min, flow rate = 0.8 mL/min, 210−400 nm). t_R = 4.37 min. HRMS (ES+) *m/e*: (M + 1) calcd for $C_{20}H_{21}F_7NO_2$, 440.1461; found, 440.1455.

2-[(Butyl{4-[2,2,2-trifluoro-1-hydroxy-1-(trifluoromethyl)ethyl]phenyl}amino)methyl]-4-(trifluoromethoxy)phenol (14). ^{1}H NMR (CD_3OD, δ): 0.98 (t, 3H), 1.42 (m, 2H), 1.67 (m, 2H), 3.50 (t, 2H), 4.57 (s, 2H), 6.74−6.88 (m, 4H), 6.98 (dd, J = 2.2, 8.6 Hz, 1H), 7.50 (d, J = 8.7 Hz, 2H). MS (ES) *m/e*: 506 (M + 1). >99% pure by HPLC (Waters symmetry shield, RPq 3.5 μm, 2.1 × 30 mm^2, H_2O (with 0.1% HCOOH)/MeOH (with 0.075% HCOOH) (50:50) to 100% MeOH (with 0.075% HCOOH) over 3.5 min, flow rate = 3.5 mL/min, 210−400 nm). t_R = 3.03 min. HRMS (ES+) *m/e*: (M + 1) calcd for $C_{21}H_{21}F_9NO_3$, 506.1378; found, 506.1372.

2-[(Butyl{4-[2,2,2-trifluoro-1-hydroxy-1-(trifluoromethyl)ethyl]phenyl}amino)methyl]-4,6-dichlorophenol (15). ^{1}H NMR (CD_3OD, δ): 0.90 (t, 3H), 1.41 (m, 2H), 1.68 (m, 2H), 3.48 (t, 2H), 4.57 (s, 2H), 6.70 (d, J = 9.0 Hz, 2H), 6.86 (d, J = 2.3 Hz, 1H), 7.25 (d, J = 2.5 Hz, 1H), 7.49 (d, J = 8.7 Hz, 2H). MS (APCI) *m/e*: 490 (M + 1). >96% pure by HPLC (Waters symmetry shield, RPq 3.5 μm, 2.1 × 30 mm^2, H_2O (with 0.1% HCOOH)/MeOH (with 0.075% HCOOH) (50:50) to 100% MeOH (with 0.075% HCOOH) over 5 min, flow rate = 0.8 mL/min, 210−400 nm). t_R = 4.89 min. HRMS (ES+) *m/e*: (M + 1) calcd for $C_{20}H_{20}Cl_2F_6NO_2$, 490.0775; found, 490.0770.

2-[(Butyl{4-[2,2,2-trifluoro-1-hydroxy-1-(trifluoromethyl)ethyl]phenyl}amino)methyl]-4-chlorophenol (16). ^{1}H NMR (CD_3OD, δ): 0.99 (t, 3H), 1.43 (m, 2H), 1.66 (m, 2H), 3.52 (t, 2H), 4.56 (s, 2H), 6.77−6.9 0 (m, 4H), 7.06 (dd, J = 2.6, 8.6 Hz, 1H), 7.54 (d, J = 8.9 Hz, 2H). MS (ES) *m/e*: 456 (M + 1). >99% pure by HPLC (Waters symmetry shield, RPq 3.5 μm, 2.1 × 30 mm^2, H_2O (with 0.1% HCOOH)/MeOH (with 0.075% HCOOH) (50:50) to 100% MeOH (with 0.075% HCOOH) over 3.5 min, flow rate = 1.5 mL/min, 210−400 nm). t_R = 2.96 min. HRMS (ES+) *m/e*: (M + 1) calcd for $C_{20}H_{20}ClF_6NO_2$, 456.1165; found, 456.1160.

4-[(Butyl{4-[2,2,2-trifluoro-1-hydroxy-1-(trifluoromethyl)ethyl]phenyl}amino)methyl]-2-chlorophenol (17). ^{1}H NMR (CD_3OD, δ): 0.96 (t, 3H), 1.39 (m, 2H), 1.61 (m, 2H), 3.50 (t, 2H), 4.53 (s, 2H), 6.83−6.99 (m, 4H), 7.13 (d, J = 1.9 Hz, 1H), 7.55 (d, J = 8.7 Hz, 2H). MS (ES) *m/e*: 456 (M + 1). >97% pure by HPLC (Waters symmetry shield, RPq 3.5 μm, 2.1 × 30 mm^2, H_2O (with 0.1% HCOOH)/MeOH (with 0.075% HCOOH) (50:50) to 100% MeOH (with 0.075% HCOOH) over 3.5 min, flow rate = 1.5 mL/min, 210−400 nm). t_R = 2.82 min. HRMS (ES+) *m/e*: (M + 1) calcd for $C_{20}H_{20}ClF_6NO_2$, 456.1165; found, 456.1160.

4-[(Butyl{4-[2,2,2-trifluoro-1-hydroxy-1-(trifluoromethyl)ethyl]phenyl}amino)methyl]-2-chloro-6-methoxyphenol (18). ^{1}H NMR (CD_3OD, δ): 0.96 (t, 3H), 1.41 (m, 2H), 1.61 (m, 2H), 3.51 (t, 2H), 3.77 (s, 3H), 4.53 (s, 2H), 6.69 (d, J = 1.7 Hz, 1H), 6.76 (d, J = 1.6 Hz, 1H), 6.89 (d, J = 9.0 Hz, 2H), 7.56 (d, J = 8.7 Hz, 2H). MS (ES) *m/e*: 486 (M + 1). >97% pure by HPLC (Waters symmetry shield, RPq 3.5 μm, 2.1 × 30 mm^2, H_2O (with 0.1% HCOOH)/MeOH (with 0.075% HCOOH) (50:50) to 100% MeOH (with 0.075% HCOOH) over 3.5 min, flow rate = 1.5 mL/min, 210−400 nm). t_R = 2.81 min. HRMS (ES+) *m/e*: (M + 1) calcd for $C_{21}H_{23}ClF_6NO_3$, 486.1271; found, 486.1265.

2-[4-(Butyl{[3-chloro-4,5-bis(methyloxy)phenyl]methyl}amino)phenyl]-1,1,1,3,3,3-hexafluoro-2-propanol (19). ^{1}H NMR (CD_3OD, δ): 0.98 (t, J = 7.2 Hz, 3H), 1.30−1.50 (m, 2H), 1.55−1.75 (m, 2H), 3.50 (t, J = 7.7 Hz, 2H), 3.78 (s, 3H), 3.79 (s, 3H), 4.56 (s, 2H), 6.82 (dd, J = 6.3, 1.7 Hz, 4H), 7.54 (d, J = 8.8 Hz, 2H). MS (ES) *m/e* = 500 (M + 1). >99% pure by HPLC (Waters symmetry shield, RPq 3.5 μm, 2.1 × 30 mm^2, H_2O (with 0.1% HCOOH)/MeOH (with 0.075% HCOOH) (50:50) to 100% MeOH (with 0.075% HCOOH) over 3 min, flow rate = 1.5 mL/min, 210−400 nm). t_R = 2.89 min. HRMS (ES+) *m/e*: (M + 1) calcd for $C_{22}H_{25}ClF_6NO_3$, 500.1427; found, 500.1421.

4-[(Butyl{4-[2,2,2-trifluoro-1-hydroxy-1-(trifluoromethyl)ethyl]phenyl}amino)methyl]-2,6-dichlorophenol (20). ^{1}H NMR (CD_3OD, δ): 0.98 (t, 3H), 1.41 (m, 2H), 1.64 (m, 2H), 3.46 (t, 2H), 4.50 (s, 2H), 6.75 (d, J = 9.1 Hz, 2H), 7.12 (s, 2H), 7.50 (d, J = 8.9 Hz,2H). MS (APCI) *m/e*: 490 (M + 1). >95% pure by HPLC (Waters symmetry shield, RPq 3.5 μm, 2.1 × 30 mm^2, H_2O (with 0.1% HCOOH)/MeOH (with 0.075% HCOOH) (50:50) to 100% MeOH (with 0.075% HCOOH) over 5 min, flow rate = 0.8 mL/min, 210−400 nm). t_R = 4.58 min. HRMS (ES+) *m/e*: (M + 1) calcd for $C_{20}H_{20}Cl_2F_6NO_2$, 490.0775; found, 490.0770.

2-{4-[Butyl(3,5-dichlorobenzyl)amino]phenyl}-1,1,1,3,3,3-hexafluoropropan-2-ol (21). ^{1}H NMR (CD_3OD, δ): 0.98 (t, 3H), 1.42 (m, 2H), 1.66 (m, 2H), 2.51 (s, 3H), 3.48 (t, 2H), 4.55 (s, 2H), 6.71 (d, J = 9.1 Hz, 2H), 7.17 (d, J = 1.5 Hz, 2H), 7.30 (s, 1H), 7.49 (d, J = 8.9 Hz, 2H). MS (APCI) *m/e*: 474 (M + 1). >99% pure by HPLC (Waters symmetry shield, RPq 3.5 μm, 2.1 × 30 mm^2, H_2O/CH_3CN (with 0.1% HCOOH) (85:15) to 100% CH_3CN over 3.5

min, flow rate = 1.0 mL/min). t_R = 4.45 min. HRMS (ES+) *m/e*: (M + 1) calcd for $C_{20}H_{20}Cl_2F_6NO$, 474.0826; found, 474.0821.

2-{4-[Butyl(3,5-dichloro-4-methoxybenzyl)amino]phenyl}-1,1,1,3,3,3-hexafluoropropan-2-ol (22). ^{1}H NMR (CD_3OD, δ): 0.98 (t, 3H), 1.41 (m, 2H), 1.64 (m, 2H), 3.48 (t, 2H), 3.85 (s, 3H), 4.55 (s, 2H), 6.74 (d, J = 9.1 Hz, 2H), 7.21 (s, 2H), 7.52 (d, J = 8.8 Hz, 2H). MS (ES) *m/e*: 504 (M + 1). >99% pure by HPLC (Waters symmetry shield, RPq 3.5 μm, 2.1 × 30 mm^2, H_2O (with 0.1% HCOOH)/MeOH (with 0.075% HCOOH) (50:50) to 100% MeOH (with 0.075% HCOOH) over 5 min, flow rate = 1.5 mL/min, 210−400 nm). t_R = 3.06 min. HRMS (ES+) *m/e*: (M + 1) calcd for $C_{21}H_{22}Cl_2F_6NO_2$, 504.0932; found, 504.0926.

LXRα and LXRβ Binding Assays. Human biotinylated LXRα and LXRβ LBDs[20] were incubated at 50 and 25 nM, respectively, with 0.25 mg/mL streptavidin-coupled LEADseeker imaging beads (GE Healthcare) in assay buffer (50 mM MOPS (pH 7.5), 50 mM NaF, 0.05 mM CHAPS, 0.1 mg/mL FAF−BSAA) for 60 min at 25 °C. After being incubated, the receptor-bead slurry was pelleted by centrifugation at 1200*g*. The supernatant was discarded, and the beads were resuspended in the original volume of assay buffer that contained freshly added 10 mM DTT with gentle mixing. D-Biotin (Pierce Chemical) was added to the resuspended receptor bead solution at 200 uM, and the mixture was allowed to incubate at room temperature for 60 min. After the incubation, [*N*-methyl-^{3}H]-GW0438[21] was added to the receptor/bead mix, and the mixture was mixed gently. The receptor/bead/radio-ligand mixture (25 μL) was added to each well of an assay plate that containined 0.5 μL of the test compound. The final test compound concentrations were between 300 pM and 20 μM. Plates were incubated at room temperature for 3 h and were then imaged on a ViewLux 1430 ultraHTS microplate imager (Perkin-Elmer).

Coactivator and Corepressor Panel Peptide Scanning. The reagents for the FRET-based cell-free peptide scanning assays were prepared as described in ref 20 with minor modifications. Europium-labeled streptavidin (12 μL, 10 nM) was added to each well of a 384-well plate that contained 1 μL of 500 nM biotinylated test peptide and was allowed to equilibrate for 30 min at room temperature. At the same time, each test compound at 10 μM was allowed to incubate for 30 min with the biotin-blocked LXR APC solution. The LXR APC test compound mixture (12 μL) was added to a plate that contained the test peptide coupled europium−streptavidin complex, was allowed to equilibrate for 1 h, and was then imaged on a ViewLux 1430 ultraHTS microplate imager (Perkin-Elmer) in time-resolved mode. The final assay volume was 25 μL. The values were normalized by log (compound activity/basal activity).

Mammalian Two-Hybrid (M2H) Assay. CV-1 cells were cultured in DME high-glucose media that was supplemented with 10% FBS and 2 mM glutamine in a humidified incubator (5% CO_2 in air) at 37 °C. 3 days Three days prior to plating for transfection, cells were harvested with 0.25% trypsin/2 mM EDTA in phenol red-free Dulbecco's phosphate-buffered saline (without calcium or magnesium) and were collected in phenol red-free DMEM-F12/15 mM HEPES medium that was supplemented with 10% charcoal/dextran-treated fetal bovine serum and 2 mM L-glutamine (experimental medium). After 3 days in culture, cells were again harvested and were suspended in experimental medium. The cells were seeded at 2.0 × 10^4 cells per well in a 96-well plate and were returned to the incubator for 24 h. Cells were then transfected by the use of Lipofectamine (Life Technologies) according to the manufacturer's instructions. The total amount of DNA that was transfected into each well was 80 ng. Transfection mixtures contained 15 ng of VP16-LXRβ plasmid, 8 ng of SPAP reporter, 25 ng of pCH110-α-gal control plasmid, 24 ng of pBluescript II KS+ (Clonetech), and 8 ng of either coactivator or corepressor plasmid. Cells were transfected for 16 h, the medium was aspirated, and 100 μL of ligand was added. We prepared appropriate ligand concentrations from DMSO stock solutions by using phenol red-free DMEM/F-12 that was supplemented with 10% heat-inactivated, delipidated, charcoal- stripped FBS. The final concentration of DMSO was 0.1%. Cells were incubated for 24 h in the presence of drug, after which the media was sampled and assayed for alkaline phosphatase activity, and the cells were assayed for α-galactosidase activity to normalize for transfection efficiency. Plates were read on a Thermomax plate reader (Molecular Devices) at 405 nm.

Transrepression, ChIP, and SUMOylation Assays. Experimental procedures were performed according to ref 17.

Supporting Information Available: ^{1}H NMR spectra for compounds **4**−**5** and **7**−**22** as well as experimental procedures for the crystallography research described in this manuscript. This material is available free of charge via the Internet at http://pubs.acs.org.

References

(1) (a) Lehmann, J. M.; Kliewer, S. A.; Moore, L. B.; Smith-Oliver, T. A.; Blanchard, D. E.; Spencer, T. A.; Willson, T. M. Activation of the nuclear receptor LXR by oxysterols defines a new hormone response pathway. *J. Biol. Chem.* **1997**, *272*, 3137–3140.

(2) Spencer, T. A.; Gayen, A. K.; Phirwa, S.; Nelson, J. A.; Taylor, F. R.; Kandutsch, A. A.; Erickson, S. K. 24(*S*),25-Epoxycholesterol. Evidence consistent with a role in the regulation of hepatic cholesterogenesis. *J. Biol. Chem.* **1985**, *260*, 13391–13394.

(3) Collins, J. L.; Fivush, A. M.; Watson, M. A.; Galardi, C. M.; Lewis, M. C.; Moore, L. B.; Parks, D. J.; Wilson, J. G.; Tippin, T. K.; Binz, J. G.; Plunket, K. D.; Morgan, D. G.; Beaudet, E. J.; Whitney, K. D.; Kliewer, S. A.; Willson, T. M. Identification of a nonsteroidal liver X receptor agonist through parallel array synthesis of tertiary amines. *J. Med. Chem.* **2002**, *45*, 1963–1966.

(4) Schultz, J. R.; Tu, H.; Luk, A.; Repa, J. J.; Medina, J. C.; Li, L.; Schwendner, S.; Wang, S.; Thoolen, M.; Mangelsdorf, D. J.; Lustig, K. D.; Shan, B. Role of LXRs in control of lipogenesis. *Genes Dev.* **2000**, *14*, 2831–2838.

(5) Rader, D. J. Liver X receptor and farnesoid X receptor as therapeutic targets. *Am. J. Cardiol* **2007**, *100*, 15N–19N.

(6) Zelcer, N.; Tontonoz, P. Liver X receptors as integrators of metabolic and inflammatory signaling. *J. Clin. Invest.* **2006**, *116*, 607–614.

(7) Collins, J. L. Therapeutic opportunities for liver X receptor modulators. *Curr. Opin. Drug Discov. Devel.* **2004**, *7*, 692–702.

(8) (a) Jaye, M. LXR agonists for the treatment of atherosclerosis. *Curr. Opin. Invest. Drugs* **2003**, *4*, 1053–1058. (b) Lund, E. G.; Menke, J. G.; Sparrow, C. P. Liver X receptor agonists as potential therapeutic agents for dyslipidemia and atherosclerosis. *Arterioscler., Thromb., Vasc. Biol.* **2003**, *237*, 1169–1177.

(9) Groot, P. H. E.; Pearce, N. J.; Yates, J. W.; Stocker, C.; Sauermelch, C.; Doe, C. P.; Willette, R. N.; Olzinski, A.; Peters, T.; d'Epagnier, D.; Morasco, O.; Krawiec, J. A.; Webb, C. L.; Aravindhan, K.; Jucker, B.; Burgert, M.; Ma, C.; Marino, J. P.; Collins, J. L.; Macphee, C. H.; Thompson, S. K.; Jaye, M. Synthetic LXR agonists increase LDL in CETP species. *J. Lipid Res.* **2005**, *46*, 2182–2191.

(10) Williams, S.; Bledsoe, R. K.; Collins, J. L.; Boggs, S.; Lambert, M. H.; Miller, A. B.; Moore, J.; McKee, D. D.; Moore, L.; Nichols, J.; Parks, D.; Watson, M.; Wisely, B.; Willson, T. M. X-ray crystal structure of the liver X receptor β ligand binding domain: regulation by a histidine-tryptophan switch. *J. Biol. Chem.* **2003**, *278*, 27138–27143.

(11) Masciadri, R.; Kamer; Matthias, N. N regioselective Friedel−Crafts alkylation of anilines and amino-substituted heteroarenes with hexafluoroacetone sesquihydrate. *Eur. J. Org. Chem.* **2003**, *21*, 4286–4291.

(12) Resche-Rigon, M.; Gronemeyer, H. Therapeutic potential of selective modulators of nuclear receptor action. *Curr. Opin. Chem. Biol.* **1998**, *2*, 501–507.

(13) de Lera, A. R.; Bourguet, W.; Altucci, L.; Gronemeyer, H. Design of selective nuclear receptor modulators: RAR and RXR as a case study. *Nat. Rev. Drug Discovery* **2007**, *6*, 811–820.

(14) Jaye, M.; Krawiec, J. A.; Campobasso, N.; Smallwood, A.; Qiu, C.; Lu, Q.; Kerrigan, J. J.; De Los Frailes Alvaro, M.; Laffitte, B.; Liu, W.-S.; Marino, J. P., Jr.; Meyer, C. R.; Nichols, J. A.; Parks, D. J.; Perez, P.; Sarov-Blat, L.; Seepersaud, S. D.; Steplewski, K. M.; Thompson, S. K.; Wang, P.; Watson, M. A.; Webb, C. L.; Haigh, D.; Caravella, J. A.; Macphee, C. H.; Willson, T. M.; Collins, J. L. Discovery of substituted maleimides as liver X receptor agonists and determination of a ligand-bound crystal structure. *J. Med. Chem.* **2005**, *48*, 5419–5422.

(15) Iannone, M. A.; Consler, T. G.; Pearce, K. H.; Stimmel, J. B.; Parks, D. J.; Gray, J. G. Multiplexed molecular interactions of nuclear

receptors using fluorescent microspheres. *Cytometry* **2001**, *44*, 326–337.

(16) Iannone, M. A.; Simmons, C. A.; Kadwell, S. H.; Svoboda, D. L.; Vanderwall, D. E.; Deng, S.-J.; Consler, T. G.; Shearin, J.; Gray, J. G.; Pearce, K. H. Correlation between in vitro peptide binding profiles and cellular activities for estrogen receptor-modulating compounds. *Mol. Endocrinol.* **2004**, *18*, 1064–1081.

(17) Ghisletti, S.; Huang, W.; Ogawa, S.; Pascual, G.; Lin, M.-E.; Willson, T. M.; Rosenfeld, M. G.; Glass, C. K. Parallel SUMOylation-dependent pathways mediate gene- and signal-specific transrepression by LXRs and PPARγ. *Mol. Cell* **2007**, *25*, 57–70.

(18) Treuter, E.; Gustafsson, J.-A. Wrestling rules in transrepression: as easy as SUMO-1, -2, -3. *Mol. Cell* **2007**, *25*, 178–180.

(19) Trump, R. P.; Cobb, J. E.; Shearer, B. G.; Lambert, M. H.; Nolte, R. T.; Willson, T. M.; Buckholz, R. G.; Zhao, S. M.; Leesnitzer, L. M.; Iannone, M. A.; Pearce, K. H.; Billin, A. N.; Hoekstra, W. J. Co-crystal structure guided array synthesis of PPARγ inverse agonists. *Bioorg. Med. Chem. Lett.* **2007**, *17*, 3916–3920.

(20) Spencer, T. A.; Li, D.; Russel, J. S.; Collins, J. L.; Bledsoe, R. K.; Consler, T. G.; Moore, L. B.; Galardi, C. M.; McKee, D. D.; Moore, J. T.; Watson, M. A.; Parks, D. J.; Lambert, M. H.; Willson, T. M. Pharmacophore analysis of the nuclear oxysterol receptor LXRα. *J. Med. Chem.* **2001**, *44*, 886–897.

(21) Noble, S. M.; Carnahan, V. E.; Moore, L. B.; Luntz, T.; Wang, H.; Ittoop, O. R.; Stimmel, J. B.; Davis-Searles, P. R.; Watkins, R. E.; Wisely, G. B.; LeCluyse, E.; Tripathy, A.; McDonnell, D. P.; Redinbo, M. R. Human PXR forms a tryptophan zipper-mediated homodimer. *Biochemistry* **2006**, *45*, 8579–8589.

JM800612U